

Monoclonal antibody 3H11 chimeric antigen receptors enhance T cell effector function and exhibit efficacy against gastric cancer

HAIBO HAN^{1*}, SHANSHAN WANG^{2*}, YING HU^{1*}, ZHAOWEI LI^{3*}, WEI YANG¹,
YUNWEI LV¹, LIMIN WANG¹, LIANHAI ZHANG³ and JIAFU JI³

Departments of ¹Biobank, ²Clinical Laboratory and ³Gastrointestinal Surgery,
Key Laboratory of Carcinogenesis and Translational Research (Ministry of Education/Beijing),
Peking University Cancer Hospital and Institute, Beijing 100142, P.R. China

Received July 6, 2017; Accepted December 29, 2017

DOI: 10.3892/ol.2018.8255

Abstract. Although chimeric antigen receptor T cell (CAR-T) therapies for certain types of solid tumors have been used in clinical trials, novel CARs that are able to target gastric cancer (GC) are still required. In our previous study, monoclonal antibody 3H11 (mAb 3H11), generated from immunization with five human GC cell lines, was demonstrated to have a 93.5% positive reaction with a clear membrane location and more than 5% cancer cell staining in GC tissues in our previous study. In the present study, 3H11-CARs were designed for modified T cell therapy. To begin with, it was confirmed that the single-chain variable fragment (scFV) of the mAb 3H11, known as scFV-3H11, exhibited similar activity with the natural antibody. In addition, scFV-3H11 CAR-T cells are able to kill tumor cells accompanied with increased interleukin-2 and interferon- γ secretion *in vitro*, and reduced the tumor burden in GC cell lines and patient-derived GC cells *in vivo*. In conclusion, scFV-3H11 CARs may have the potential to treat mAb 3H11-positive GC.

Introduction

Gastric cancer (GC) is the third leading cause of cancer-associated mortality worldwide (1). Statistics from the National Central Cancer Registry of China revealed that

GC, with ~498,000 associated mortalities in 2015, is the second most common cause of cancer-associated mortality in China (2). Due to the fact that >80% of GC cases are diagnosed in the middle-late stages, there is a <25% 5-year survival rate in these patients (3). The efficacy of adjuvant chemotherapy, the main treatment for advanced GC, is limited due to its non-specific anticancer activity. Therefore, cellular antitumor strategies, including activated dendritic cells, tumor-infiltrating lymphocytes and, particularly, genetically engineered T lymphocytes, have demonstrated potential for the treatment of solid tumors (4).

Chimeric antigen receptors (CARs), which are responsible for the success of T-cell immunotherapy, contain three main elements; an extracellular domain, a single-chain antigen-recognition domain (usually an scFv) and a transmembrane domain. ScFv recognizes and binds to a specific tumor antigen independently of major histocompatibility complex molecules, while the transmembrane domain is an intracellular signaling domain including a signal-transduction molecule of the T cell receptor [usually cluster of differentiation (CD)3 ζ] and costimulatory receptors (e.g., CD137, CD28 or OX40) (5). For hematological tumors, CD19-, CD20- and CD22-targeted CAR-T cell treatments have completed clinical trials and have displayed notable antitumor activity (4). Previous studies have reported that CD19-specific CAR-T-cell treatment had been the most effective therapy with complete response (CR) rates of 70-90% (6). For solid tumors, a series of CARs targeting 23 different antigens, including prostate-specific membrane antigen, fibroblast activation protein and GD2, had been constructed and validated in clinical trials (4). As for GC, CARs targeting carcinoembryonic antigen, mucin 1 and receptor tyrosine-protein kinase erbB-2 remain in clinical trials (4). Considering the heterogeneity of GC cells, the identification of novel antigen-based CAR-T cells for the treatment of GC is urgently required.

Previously, a monoclonal antibody, mAb-3H11, was obtained using the hybridoma technique with spleen cells from mice immunized with five human GC cell lines (7). Briefly, Balb/c mice were immunized with one of the following human GC cell lines: M85, SGC7901, Kato III or MGC-803 once a week, and were mice were injected with MKN45 cells at the middle of each week by intra-splenic injection. Spleen cells

Correspondence to: Dr Limin Wang, Department of Biobank, Key Laboratory of Carcinogenesis and Translational Research (Ministry of Education/Beijing), Peking University Cancer Hospital and Institute, 52 Fucheng Road, Beijing 100142, P.R. China
E-mail: wanglimi100@126.com

Dr Jiafu Ji, Department of Gastrointestinal Surgery, Key Laboratory of Carcinogenesis and Translational Research (Ministry of Education/Beijing), Peking University Cancer Hospital and Institute, 52 Fu-Cheng Road, Beijing 100142, P.R. China
E-mail: jijiafu@hsc.pku.edu.cn

*Contributed equally

Key words: chimeric antigen receptor, immunotherapy, adoptive T cell therapy, gastric cancer

from mice immunized with GC cells were harvested and fused (via membrane fusion) with the murine myeloma SP2/0 cells using the cell fusion hybridoma technique. Candidate hybridoma cells producing mAbs were obtained by selective culture and ELISA screening in GC cells. Among all candidate antibodies, mAb-3H11 was confirmed to exhibit a high specific binding capacity to GC cells and a reaction rate of ~93.5% in human GC tissues; however, it did not react with normal cells (7). Furthermore, it was also determined whether mAb 3H11 reacted with normal human organ tissue, including heart, liver, spleen, lung, kidney, stomach, colon, brain, bone, muscle, skin and nerve (7). As a result, there was only a weak positive reaction rate for mAb-3H11 in 1/15 normal gastric mucosa and a weak cross-reaction with salivary gland, sweat gland, bronchus and intestinal content (7). The above results suggested that mAb 3H11 reacted with most GC tissues, but reacted weakly with the few of normal tissues, indicating that mAb 3H11 has potential for GC diagnosis or target therapy.

Furthermore, I¹³¹-labeled or I¹²⁵-labeled mAb 3H11 indicated a high sensitivity and specificity for intraoperative detection of the lymphatic micrometastasis in two clinical trials for radioimmunoguided surgery (8,9), suggesting its potential application as a radioiodination reagent to detect metastatic cancer in clinical practice. In addition, our previous study also confirmed the sequences of variable region heavy chain (V_H) and light chain (V_L) for mAb-3H11 (10). The antigen of mAb-3H11 was previously reported to be centrosomal protein 290 (CEP290) by cDNA library screening (11); however, the intracellular location of CEP290 and predominant membrane location of the antigen of mAb 3H11 remain unclear.

The present study not only designed lentivirus-mediated scFv-3H11 CAR-harboring CD28, CD137 and CD3 ζ signaling domains, but also evaluated the antitumor activity of CAR-T cells against GC cells both *in vitro* and *in vivo*. The results of the present study provide information for future clinical trials testing the use of this CAR-T cell immunotherapy for patients with GC.

Materials and methods

Cell culture. The human GC cell lines, NCI-N87, MKN45, AGS, NUGC3, SGC7901, MGC803 and BGC823, and Jurkat cells, were obtained from the Cell Center of Peking Union Medical University (Beijing, China). All GC cells and Jurkat cells were cultured in RPMI-1640 medium (Gibco; Thermo Fisher Scientific, Inc., Waltham, MA, USA) containing 10% fetal bovine serum (Gibco; Thermo Fisher Scientific, Inc.) and incubated at 37°C in a humidified incubator.

Isolation of primary GC cells. Two cases of primary human GC cells (name as -1 and PGCC-2) were surgically obtained via tumor resection from a 62 year old male and a 64-year-old male in October 2013 (Peking University Cancer Hospital and Institute, Beijing, China). All samples were mechanically cut into 1 mm pieces using scissors, and digested with 1 mg/ml collagenase I and 1 mg/ml collagenase IV (Thermo Fisher Scientific, Inc.) at 37°C for 1 h. Subsequently, PGCCs were cultured in F-12 nutrient mixture (Ham)-Dulbecco's modified Eagle's medium (Invitrogen; Thermo Fisher Scientific, Inc.) for

conditional reprogramming and immortalization of epithelial cells as previously described (12). Written informed consent had obtained from all patients enrolled in the present study and all protocols were approved by the Peking University Cancer Hospital and Institute Ethical Committee.

RNA extraction and overlap extension-polymerase chain reaction (OE-PCR). Total RNA was extracted from hybridoma-3H11 cells using an RNeasy Mini kit (Qiagen, Inc., Valencia, CA, USA), according to the manufacturer's protocols. A total of 2 μ g RNA was reverse transcribed using TransScript[®] All-in-One First-Strand cDNA Synthesis SuperMix (Beijing TransGen Biotech Co., Ltd., Beijing, China) according to the manufacturer's protocol. The annealing temperature was designed on the basis of our previous study (10). V_H and V_L were amplified by PCR using the following thermocycling conditions: Pre-denaturation at 94°C for 5 min, followed by 94°C 30 sec, 45°C for 60 sec, 72°C for 90 sec for 30 cycles and finally, 72°C for 10 min and 4°C for 1 min. The sequences for primers were V_H-forward, 5'-GAATTCCAGGTTTCAGCTGTG-3' V_H-reverse-1, 5'-TGAGGAGACGGTGACTGAGG-3' and V_H-reverse-2, 5'-CGATCCGCCACCGCCAGAGCCACC TCCGCCTGAACCGCTCCACCTGAGGAGACGGTGAC TGAGG-3'; V_L-forward-1, 5'-GGTGGAGGCGGTTTCAGGC GGAGGTGGCTCTGGCGGTGGCGGATCGCAAATTGTA CTCACCCAGTC-3', V_L-forward-2, 5'-CAAATTGTACTC ACCCAGTC-3' and V_L-reverse, 5'-CTCGAGTTTTATTTC CAGCTTG-3'. Underlined sequences indicate the overlap linker (Gly4Ser)₃ sequence.

CDR analysis by IgBLAST. V_H and V_L OE-PCR products were cloned into PCR-blunt vectors (Invitrogen; Thermo Fisher Scientific, Inc.), sequenced by SinoGenoMax Co., Ltd. (Beijing, China) and analyzed by the IgBLAST program (13) using ImmunoGeneTics databases (<http://www.imgt.org/>).

Constructs and lentiviral packaging. The scFv-3H11 sequence, connecting the V_H and V_L using a (Gly4Ser)₃ polypeptide linker, was obtained by OE-PCR and was subsequently constructed in pEGFPN1 and plenti6-TR expression vectors. The structures of recombinant plasmids are presented in Fig. 1A and B. A signal peptide from the CD8 family, CD8SP, was added prior to the scFv-3H11 sequence. The entire DNA sequence of 3H11-CAR contained scFv-3H11, human CD8 hinge, a transmembrane domain, and CD28 and CD137 co-stimulatory and CD3 ζ signaling domains (Fig. 1B). In order to verify transduction efficiency, a tag of Myc was added immediately after the carboxyl terminus of the scFv-3H11. A lentiviral shuttle plasmid containing luciferase reporter, pELNS-Luciferase-IRES-Neo, was used to establish stable luciferase expression in GC cell lines in order to detect cytotoxicity. Viral particles were produced using transfection into package HEK-293FT cells with a four-plasmid system and were purified using PEG-it[™] Virus Precipitation Solution (Stratex Scientific Ltd., Newmarket, UK). All the recombinant constructions were confirmed by sequencing (data not shown).

Secretory expression of scFv-3H11-green fluorescent protein (GFP). The pEGFPN1-CD8SP-ScFv-3H11 plasmid was

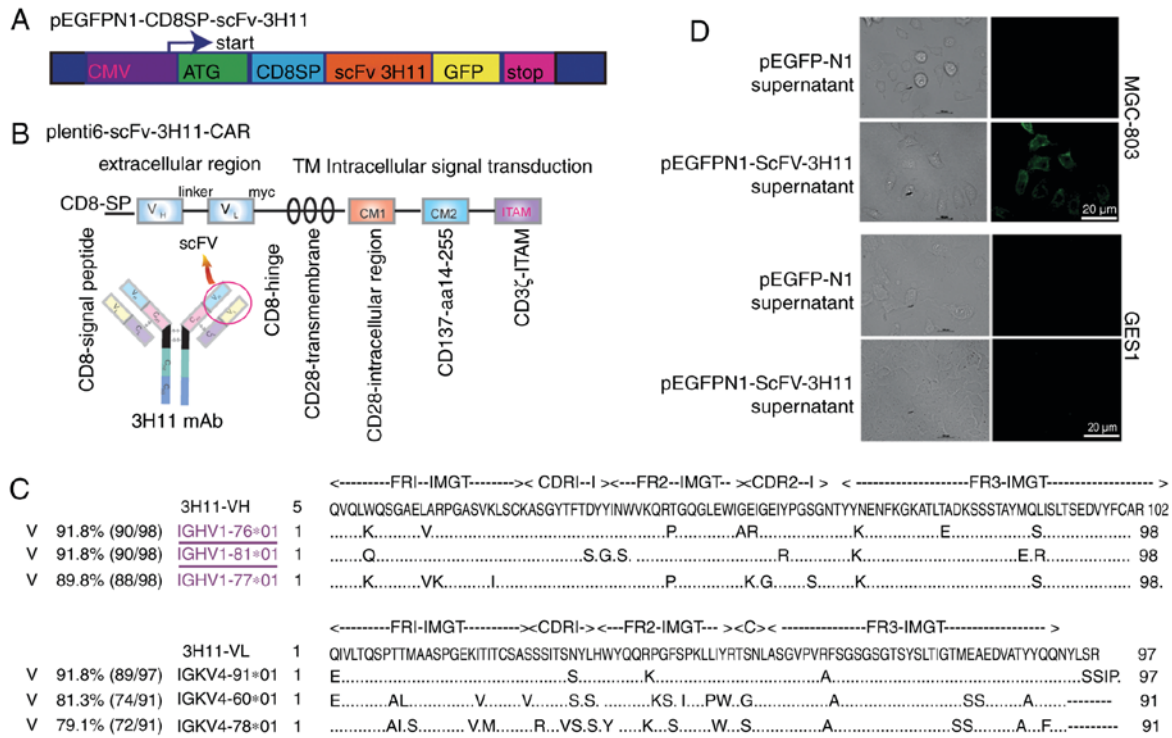


Figure 1. Structure of scFv-3H11-associated constructs and the activity analysis of scFv-3H11. Schematic diagram of (A) pEGFPN1-scFv-3H11 and (B) scFv-3H11-based 3rd-G CARs. (C) The deduced amino acid sequences of VH and VL were submitted to the online IgBLAST database. (D) Immunofluorescence staining was used to analyze the binding activity of recombinant scFv-3H11 in the medium of COS-7 cells transfected with pEGFPN1-CD8SP-scFv-3H11-GFP plasmids. CARs, chimeric antigen receptors; TM, transmembrane; IMGT, the international ImMunoGeneTics information system; CDR, the complementarity determining region; FR, frame region.

transfected into COS-7 cells at 80-90% confluence using Lipofectamine reagent (Invitrogen; Thermo Fisher Scientific, Inc.), according to manufacturer's protocols. Two days later, the culture medium containing secretory expression of recombinant scFv-3H11 was collected for analysis of activity.

Generation and expansion of 3H11-CAR T cells from peripheral blood mononuclear cells (PBMCs). PBMCs from healthy donors were purified using lymphocyte separation medium (Beijing Solarbio Science & Technology Co., Ltd., Beijing, China) by density gradient centrifugation at 1,360 x g for 20 min in room temperature. CD3⁺ T cells in PBMCs were enriched using the EasySep™ Human T Cell Isolation kit (Stemcell Technologies, Inc., Vancouver, BC, Canada), activated using Dynabeads® Human T-Expander CD3/CD28 (Thermo Fisher Scientific, Inc.) and expanded in OpTmizer™ T-Cell Expansion medium (Thermo Fisher Scientific, Inc.), containing interleukin (IL)-2 (300 U/ml; Sigma-Aldrich; Merck KGaA, Darmstadt, Germany). Lentivirus infection efficiency of the CAR-T cells was evaluated by fluorescence-activated cell sorting (FACS) analysis on day 10 prior to the first treatment.

Flow cytometry analysis. Live cells were incubated with mAb-3H11 (made in our laboratory by affinity-purification from mouse ascites using sepharose protein A; 1 µg/µl; 1:100 dilution) or an anti-Myc (1:100 dilution; cat. no. ab32; Abcam, Cambridge, UK) antibody at 37°C for 20 min, prior to being incubated with fluorescein isothiocyanate (FITC)-labeled goat anti-mouse secondary antibodies (cat no. 115-095-003;

1:100 dilution; Jackson ImmunoResearch Laboratories, Inc., West Grove, PA, USA) at 37°C for 20 min, followed by analysis on a BD Accuri C6 Cytometer using C6 software (version 1.0.264.21; BD Biosciences, Franklin Lakes, NJ, USA).

Cytotoxicity assays and cytokine secretion assays. BGC-823 and NCI-N87 cells were mixed directly with lentivirus-containing luciferase reporter for 48 h (Shanghai GeneChem Co., Ltd., Shanghai, China) and then screened by G418 for ~2 weeks to establish stable firefly luciferase-expressing cancer cells in order to detect cytotoxicity. Firefly luciferase activity in the cells (representing the live cell numbers) were measured using a Luciferase Reporter assay (Promega Corporation, Madison, WI, USA) according to the manufacturer's protocol. Mock T cells were used as the control group to normalize luciferase data for CAR-T cells, and cell lysis was calculated using the following formula: Cell lysis (%) = (1-luciferase experiment/luciferase control) x100. The specific *in vitro* antitumor activity of CAR-T cells was performed. Briefly, different types of target cells (with luciferase reporter gene) were seeded onto triplicate 96-well plates, at a density of 10³ cells/well, with 50 µl RPMI-1640 (Gibco; Thermo Fisher Scientific, Inc.). Subsequently, an equal volume of effector cells or control medium was added to each well to ensure an effector-target ratio (E/T ratio) of 25:1, 12.5:1, 6.2:1, 3.1:1, 1.6:1, or 0.8:1. Following an 8-h incubation, cell supernatants were obtained by centrifugation at 800 x g for 10 min at room temperature and collected for cytokine measurements of IL-2 and interferon (IFN)-γ concentrations using an ELISA

kit (BioLegend, Inc., San Diego, CA, USA), according to the manufacturer's protocols.

Xenograft mouse model of GC. Ten NOD/SCID mice (male; 7 weeks old; 18–20 g) were purchased from Vital River Laboratories Co., Ltd. and were housed in a pathogen-free animal housing facility at Beijing University Cancer Hospital and Institute at $23\pm 3^{\circ}\text{C}$, a relative humidity of $\sim 50\%$, 12 h light/dark cycle and a standard sterilized rodent diet from Vital River Laboratories Co., Ltd (Beijing, China) and sterilized water *ad libitum*. The animal experiments were approved by the Animal Ethics Committee of Peking University Cancer Hospital and Institute. A total of $100\ \mu\text{l}\ 1\times 10^6$ 3H11-antigen-positive MGC-803 cells, were injected subcutaneously into NOD/SCID mice on day 0. Tumor-bearing mice were randomly assigned to the CAR-T cell and control T cell groups prior to treatment, with five mice in each group. The tumor volume (TV) of each mouse was measured twice weekly using a vernier caliper and was calculated according to the following formula: $\text{TV} = 1/2 \times \text{length} \times \text{width}^2$. On day 14, when the mean TV reached $\sim 100\ \text{mm}^3$, $200\ \mu\text{l}\ 2\times 10^7$ CAR-T cells or control T cells, were infused into the tumors of the mice twice weekly by multipoint injection.

Immunohistochemical examinations. Humane endpoints were used in accordance with Peiking University Cancer Hospital and Institute standard operating protocols. Tumor tissue samples from sacrificed mice on the 35th day, according to the humane endpoints of diameter of the tumor mass (i.e., greater than 1.5 cm diameter in mice) were fixed in 10% formaldehyde solution for 24 h, dehydrated in ethyl alcohol, and embedded in paraffin, prior to being cut into $6\ \mu\text{m}$ thick sections using a microtome. Immunohistochemical (IHC) staining was performed according to standard procedures. Briefly, slides were immersed in xylene to remove paraffin, washed in a graded series of ethanol, immersed in citrate buffer at pH 6.0 and then incubated in a high-pressure sterilization oven for antigen retrieval at 100°C for 3 min. Endogenous peroxidase activity was blocked in a blocking solution with 3% H_2O_2 in PBS for 10 min at room temperature, and then the slides were incubated with PBS containing 1% bovine serum albumin (Amresco, Solon, OH, USA) for 10 min at room temperature to block non-specific binding. The tissue sections were incubated at room temperature for 1 h with a primary rabbit anti-human CD3 antibody (1:200; cat. no. ab5690; Abcam), followed by incubation with horseradish peroxidase-conjugated goat anti-mouse IgG (1:500; cat no. A4416; Sigma-Aldrich; Merck KGaA) for 1 h at room temperature. Then, the slides were visualized with 0.1% 3,3-diaminobenzidine (Sigma-Aldrich; Merck KGaA) for 2 min, and counterstained with one drop of 1% hematoxylin for 10 min at room temperature.

Statistical analysis. Statistical analyses were performed using Prism V5.00 for Windows (GraphPad Software, Inc., La Jolla, CA, USA). The differences between two groups were assessed using independent samples t-test. Dunnett's multiple comparison tests were used to compare differences between treatment groups and the control group following one-way analysis of variance. $P < 0.05$ was considered to indicate a statistically significant difference.

Results

Plasmid construction and analysis for CDR of V_H and V_L of mAb-3H11 using the IgBLAST database. The structures of recombinant plasmids are presented in Fig. 1A and B. In order to determine the secretory expression of scFv-3H11, a signal peptide from the CD8, named CD8SP, was added before the scFv-3H11 sequence. The entire DNA sequence of 3H11-CAR contained scFv-3H11, human CD8 hinge, a transmembrane domain, and CD28 and CD137 co-stimulatory and CD3 ζ signaling domains (Fig. 1B). In order to verify transduction efficiency, a Myc tag was added immediately after the carboxyl terminus of scFv-3H11. The deduced amino acid sequences of V_H and V_L were submitted to the online IgBLAST database, and were aligned to maximize the homology with the $I_G\text{HV1-76}$ and $I_G\text{KV4-91}$, respectively (Fig. 1C). The complementarity determining regions (CDRs) for the heavy and light chains of mAb-3H11 are presented in Fig. 1C.

Secretory scFv-3H11 indicated good binding activity. The binding activity of scFv-3H11 in the cultured medium of COS-7 cells was detected by live cell staining. As demonstrated in Fig. 1D, the secretory scFv-3H11 antibody in the harvested medium from COS-7 cells clearly stained the protein on the membrane of MGC-803 cells, but not of GES-1 cells. This result suggested that recombinant scFv-3H11 protein had good binding activity, similar to that of the natural antibody.

The antigens of mAb-3H11 were highly expressed in GC cells. FACS was used to assess the surface expression of 3H11-antigen proteins in a series of human GC cell lines (GCCLs), including NCI-N87, MKN45, AGS, NUGC3, SGC7901, MGC803 and BGC823 cells, and in PGCCs obtained from two patients with GC. The results of the present study suggested that 3H11-antigen was highly expressed in all the GCCLs, with the positive percentage ranging between 56.6 and 99.6%, and in the PGCCs from patient 1 (PGCC-1) with a positive percentage of 87.0% and patient 2 (PGCC-2) with a positive percentage of 50.8% (Fig. 2), while the positive percentage was only 0.9% in normal gastric epithelial GES1 cells. Therefore, mAb-3H11 demonstrated a 50.8 to 99.6% positive reaction with GC cells. NCI-N87 with a 56.6% positive rate and a BGC823 positive rate of 98.9% were selected for further study.

scFV-3H11-CAR T cells killed GC cells accompanied with an increased expression of IL-2 and IFN- γ ex vivo. Following lentivirus infection, the transduction efficiency of scFV-3H11-CAR in Jurkat cells was 51.6% (Fig. 3A), and the cytotoxicity of CAR-Jurkat cells exhibited higher average killing activity against BCG823 cells ($64.6\pm 2.7\%$; Fig. 3B) and NCI-N87 cells ($54.6\pm 2.7\%$; Fig. 3C) than did mock Jurkat cells with a low rate of lysis activity at a ratio of 25:1 E/T against BCG823 cells and NCI-N87 cells. Additionally, a dose-dependent cell killing was also performed, as demonstrated in Fig. 3B and C, and it was revealed that the cytotoxicity of scFV-3H11-CAR Jurkat cells increased as the E/T ratio increased. As for the human normal gastric epithelial GES1 cell line, there was no significant killing effect for the CAR Jurkat cells compared with the mock Jurkat cells (Fig. 3D).

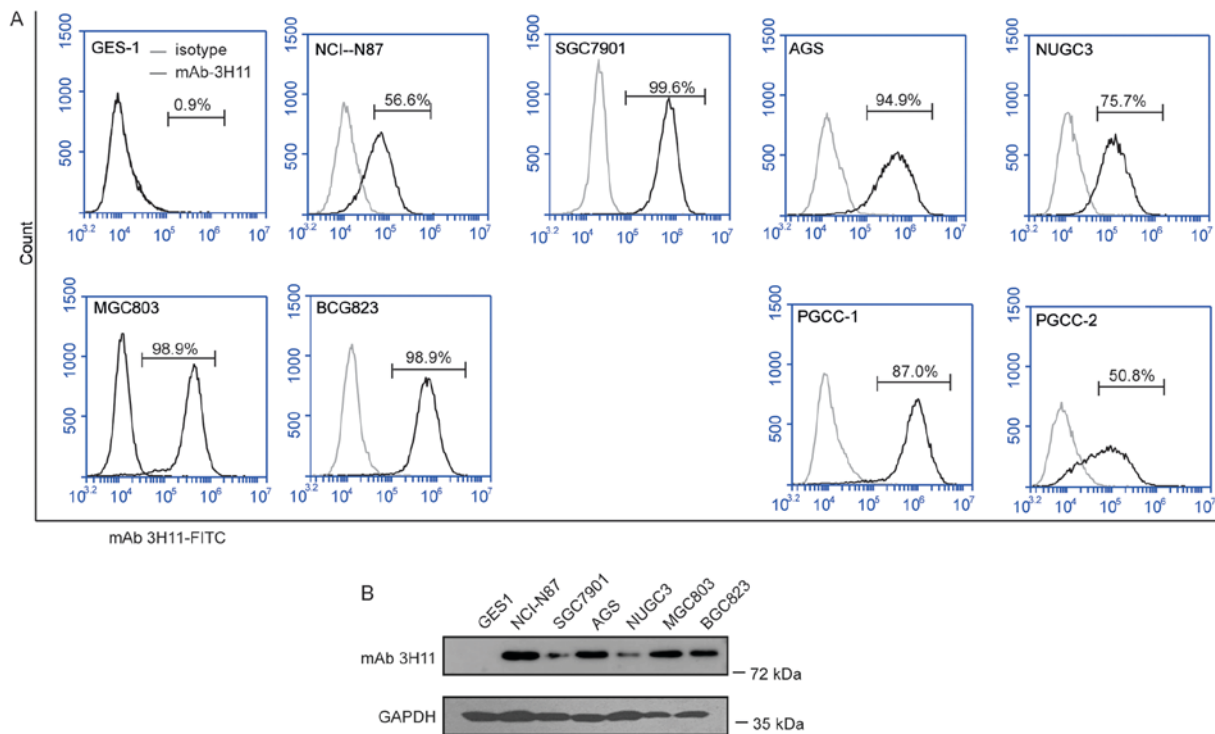


Figure 2. Analysis of the antigen expression of mAb-3H11 in GC cell lines. (A) Flow cytometry histogram plots of the surface antigen expression of mAb-3H11 in GES1 cells, MGC803, NUGC3, MKN45, NCI-N87, BCG823, MGC7901 and AGS cell lines, and two patient-derived GC cell lines. (B) Western blot analysis of the antigen expression of mAb-3H11 in GES1, NCI-N87, MGC7901, AGS, NUGC3, MGC803 and BCG823 cells. mAb, monoclonal antibody; GC, gastric cancer; PGCC, primary human GC cells.

Similarly, following lentivirus infection, the transduction efficiency of 3H11-CAR-T cells from healthy donors was 62.3% (Fig. 3E). The cytotoxicity of 3H11-CAR-T cells exhibited higher average killing activity against BGC823 cells ($79.2 \pm 1.5\%$; Fig. 3F) and NCI-N87 cells (Fig. 3G, $62.8 \pm 3.3\%$) than did mock T cells with a low rate of cell lysis at a ratio of 25:1 E/T, and the cytotoxic effects displayed a dose-dependent pattern ($P < 0.05$; Fig. 3F and G). As for the GES1 cells, the CAR-T cells had no significant killing effect, compared with the mock T cells (Fig. 3H). Furthermore, following the incubation, the levels of cytokines released by scFV-3H11-CAR T cells, including IL-2 and IFN- γ , were significantly elevated in the supernatants of BGC823 and NCI-N87 cells compared with those of the mock T cells, and the cytokine level also exhibited a dose-dependent pattern (Fig. 3I and K for IL-2 expression; Fig. 3J and L for IFN- γ expression).

scFV-3H11-CAR-T cells exhibited effective antitumor activity against xenografts. The subcutaneous xenotransplanted tumor model of GC BGC823 cells were established in NOD/SCID mice in order to determine the antitumor capacity of scFV-3H11-CAR-T cells *in vivo*. As demonstrated in Fig. 4A, treatment with CAR-T cells was performed on day 14, when the mean tumor volume (TV) had reached $\sim 100 \text{ mm}^3$ by multi-point intra-tumor injection with effector cells twice a week. In the present study, all animals presented with only one tumor. In the mouse model, the tumor weight was considerably inhibited by treatment with 3H11-CAR-T cells, while tumors in the control group continued to grow rapidly following injection with mock T cells (Fig. 4B). When the mice were sacrificed at 35 days, the mean BGC823 tumor weight in the 3H11-CAR-T

group was 176 mg, while that in the mock T group was 631 mg ($P = 0.01$; Fig. 4C and D), suggesting a 72.1% suppression in tumor weight following 3H11-CAR-T therapy in BGC823 cells. In order to assess the infiltration of 3H11-CAR-T cells, IHC labeling for CD3 T cells was performed on tumor samples initiated from BGC823 cells. The results of the present study demonstrated a considerable increase in human CD3⁺ T cells in the experimental group, while only a small number of CD3⁺ T cells were observed in the mock T group (Fig. 4E). These findings suggested that 3H11-CAR-T cells may effectively inhibit tumor growth. The results for the PGCC-1 cells were similar (data not shown).

Discussion

The high effectiveness and low toxicity of CAR-T cell therapy is primarily dependent upon the specificity of the target antigen. In our previous study, mAb-3H11 exhibited a positive reaction with five immunized GC cell lines and a negative reaction with lymphocytes, red blood cells, bone marrow cells and diploid fibroblasts. Furthermore, it also exhibited a high positive reaction rate of $\sim 93.5\%$ in tissues of all histopathological types of GC, including well-differentiated, poorly differentiated, mucosal and metastatic GC (7). The aforementioned study also detected the reactivity of mAb 3H11 in 32 types of normal human tissue, including heart, liver, spleen, lung, kidney, stomach, colon, brain, bone, muscle, skin and nerve, and the results demonstrated that there were weak positive reaction rates for mAb-3H11 with 1/15 normal gastric mucosa and a weak cross-reaction with salivary gland, sweat gland, bronchus and intestinal content (7). These previous results suggested that

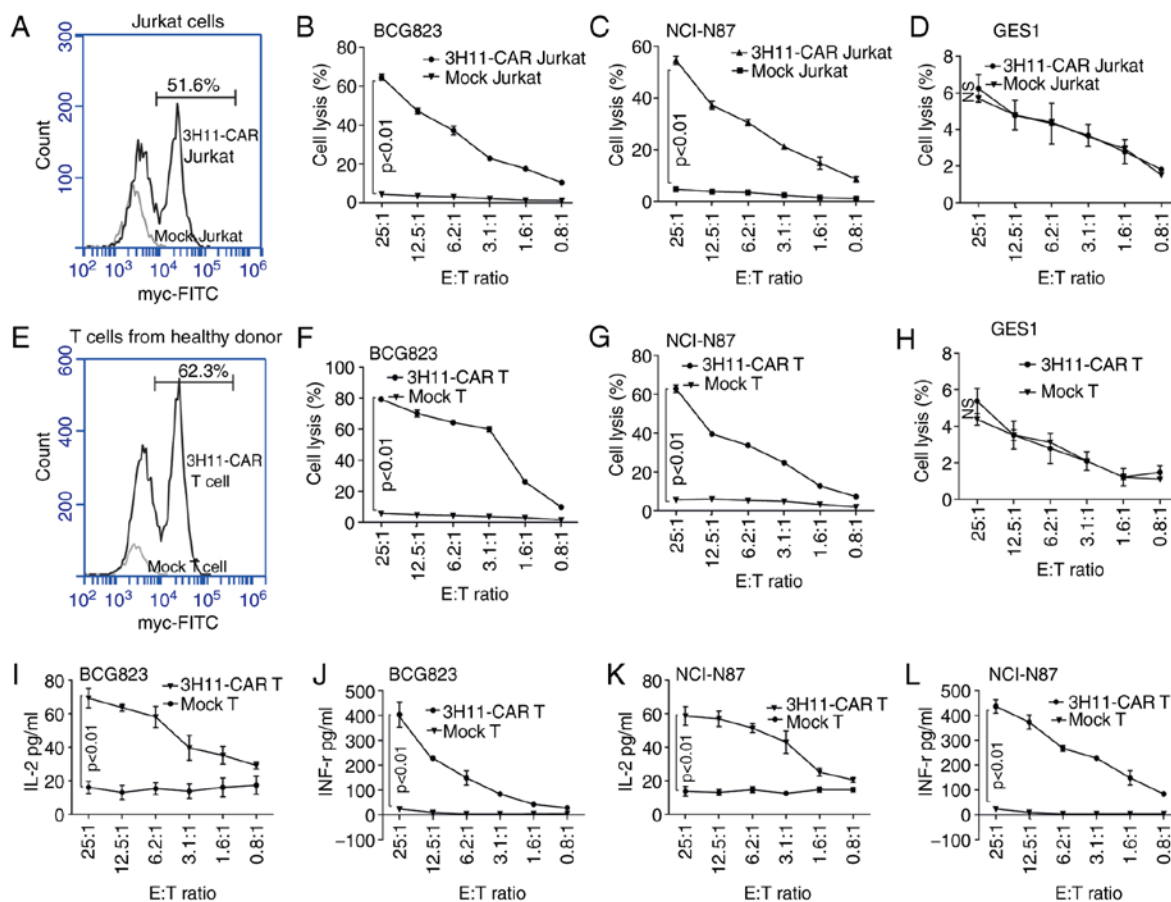


Figure 3. scFV-3H11-CAR-T cells mediate robust cytotoxicity, and IL-2 and IFN- γ production against antigen positive gastric tumor cells. (A) Flow cytometry histogram plots of 3H11-CAR lentivirus transduction efficiency for 3H11-CAR in Jurkat cells using anti-Myc antibody staining. Cytotoxicity assays were performed to measure the specific lysis of (B) BCG-823, (C) NCI-N87 and (D) GES1 cells by scFV-3H11-CAR T Jurkat cells or mock Jurkat cells for 8 h at different E/T ratio. (E) Flow cytometry histogram plots of 3H11-CAR lentivirus transduction efficiency for 3H11-CAR in CD3⁺ T cells from healthy donors using anti-Myc antibody staining. Cytotoxicity assays were performed to measure the specific lysis of (F) BCG-823, (G) NCI-N87 and (H) GES1 cells by scFV-3H11-CAR T cells or mock T cells for 8 h at different E/T ratios. Measurements of IFN- γ production in (I) BCG823 and (J) NCI-N87 cells at different E/T ratios for 8 h, as determined by ELISA. Measurements of IL-2 production in (K) BCG823 and (K) NCI-N87 cells at different E/T ratios for 8 h, as determined by ELISA. Data in (B-D and F-L) are presented as the mean \pm standard error of the mean from three independent experiments with triplicate wells. Data in (B-D and F-L) were analyzed by one-way analysis of variance. CAR, chimeric antigen receptor; IL-2, interleukin 2; IFN- γ , interferon γ ; ns, not significant.

mAb-3H11-based CAR-T cell therapy was feasible because it had little on-target, off-tumor toxicity resulting from the shared antigens in normal tissues. Therefore, in the present study, CAR-T cells were created using a single-chain variable fragment (scFv) of mAb-3H11 in order to kill GC. The results of the present study suggested that 3H11-CAR-T cells induced robust T cell cytotoxicity and elicited high levels of IL-2 and IFN- γ production compared with control CAR T cells.

The signaling region of the first-generation (1st-G) CAR mimics T cell receptor (TcR) signaling by fusing the antigen-binding region to the CD3- ζ chain, and the second-generation (2nd-G) CAR mimics TcR and costimulatory signaling by adding, for example, CD28 or CD137 domains to the intracellular region, while the third-generation (3rd-G) CAR has two costimulatory domains fused with the TcR CD3- ζ chain (14). The results of a previous study demonstrated that the 3rd-G CAR-T cells exhibited superior activation and proliferation capacity compared with the 2nd-G CAR-T cells carrying only one costimulatory domain (15). In the present study, in order to obtain the optimal antitumor effect, lentivirus-expressing scFV-3H11 3rd-G CAR was constructed. With regards to the killing mechanism of effector T cells on

target tumor cells, a previous study suggested that CARs were hybrid proteins consisting of an antigen specific binding domain (usually scFv) fused to intracellular T-cell activation domains (CD28 and CD137/CD3 ζ receptor), and CAR-expressing engineered T lymphocytes may directly recognize and kill tumor cells expressing its antigen in an human leukocyte antigen-independent manner (16). Another previous study suggested that it was possible that antigen-targeted CAR-T cells may not only efficiently kill single tumor targets, but may also kill multiple tumor targets in a sequential manner (17).

Jurkat cells are an immortalized line of human T lymphocyte cells established in the late 1970s from the peripheral blood of a 14-year-old boy (18). They have been successfully used in the evaluation of *in vitro* effectiveness of certain CAR-T cell therapies (19-22). To the best of our knowledge, the present study was the first to examine the cytotoxicity of scFV-3H11 CAR Jurkat cells *in vitro*, and it was revealed that scFV-3H11 CAR Jurkat cells killed more than half of the GC cells at a ratio of 25:1 E/T. Subsequently, 3H11-CAR were transduced into primary T cells and their antitumor effects both *in vitro* and *in vivo* were detected. The results of the present study suggested that scFV-3H11 CAR-T cells not only killed 62.8% NCI-N87

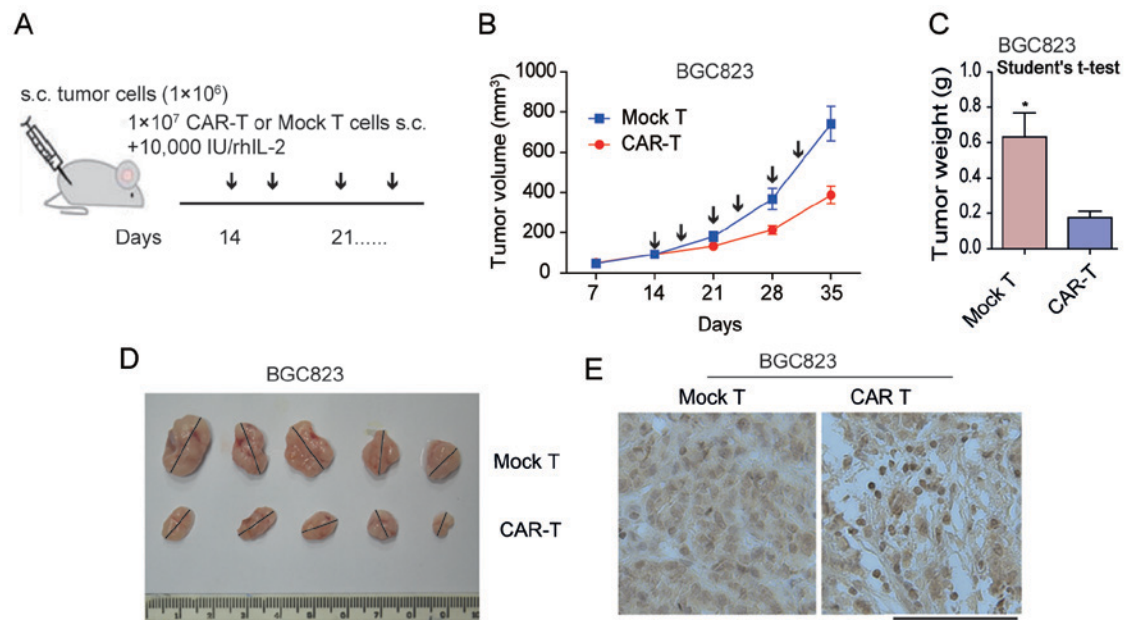


Figure 4. scFV-3H11-CAR T cells reduced tumor burden in a BGC823 gastric cancer model *in vivo*. (A) Schematic diagram of CAR T cell therapy. When the mean tumor volume reached ~ 100 mm³ on day 14, intro-tumor injection with CAR-T cells or mock T cells were performed. (B) The tumor volume for CAR-T cell and mock T cell treatment mice. Data are presented as the mean + SD (mm³) for each group. Arrows indicate the time points of injection with CAR-T or mock-T cells. (C) Tumor weight following sacrifice on day 35. Student's t-test, *P=0.01. (D) Mice were sacrificed on day 35 with maximum tumor diameters >1.5 cm. The tumor weight data are presented as the mean + SD (g) for CAR-T cell and mock T cell treated mice. (E) Immunohistochemical staining for anti-cluster of differentiation 3 was performed on tumor samples from sacrificed mice. Scale bar indicates 100 μ m. s.c., subcutaneous; CAR, chimeric antigen receptor; SD, standard deviation.

cells and 72.9% BGC823 cells at a ratio of 25:1 E/T *in vitro*, but also inhibited 72.1% tumor growth of BGC823 and 57.1% tumor growth of PGCC-1 cells *in vivo*.

The ideal delivery method of CAR-T cell therapy in solid tumors was by intravenous infusion. For the treatment of xenografts in the mouse model used in the present study, CAR-T cells were first administered by tail intravenous injection. However, little therapeutic activity was detected following treatment (data not shown). Considering that unsuccessful intravenous injection was possibly due to the poor ability of infused CAR-T cells to reach tumor-specific sites, the tumor-bearing mice were administered with an intra-tumor injection of CAR-T cells or mock T cells, and revealed that the therapeutic efficacy was improved significantly. These results were consistent with those of previous studies for T cell therapy in animal models (23-25), which had exhibited no effect by systematic infusion. Although scFv-3H11 CAR-T cells did not overcome the current barriers of CAR-T cell therapy in GC in the present study, the changes in protein levels in cultured CAR-T lymphocytes, including increased expression of chemokine receptors (26) or heparanase (27), may promote tumor infiltration and antitumor activity. Therefore, the development of 3H11-CAR-T cells co-expressed with heparanase or chemokine receptors may be a way to improve the efficacy of this therapeutic tool in the treatment of GC.

Acknowledgements

Not applicable.

Funding

This study was supported by the Beijing Committee of Science and Technology in China (grant no. D131100005313010),

the National High Technology Research and Development Program of China (863 Program; grant no. 2014AA020603), the National Natural Science Foundation of China (grant nos. 81201964, 81772632 and 81773144), Peking University (PKU) 985 Special Funding for Collaborative Research with PKU Hospitals (2013-11-20) and the interdisciplinary medicine Seed Fund of Peking University (grant no. BMU2018MX019).

Availability of data and materials

The datasets used and/or analyzed during the current study are available from the corresponding author on reasonable request.

Authors' contributions

HH, SW, YH, and ZL performed most experiments. WY and YL participated in the *in vitro* study. LW, LZ and JJ designed the experiments and coordinated the project.

Ethics approval and consent to participate

Written informed consent was obtained from all patients enrolled in the present study and all protocols were approved by the Peking University Cancer Hospital and Institute Ethical Committee.

Consent for publication

Patients provided written informed consent for the publication of their data.

Competing interests

The authors declare that they have no competing interests.

References

- Torre LA, Bray F, Siegel RL, Ferlay J, Lortet-Tieulent J and Jemal A: Global cancer statistics, 2012. *CA Cancer J Clin* 65: 87-108, 2015.
- Chen W, Zheng R, Baade PD, Zhang S, Zeng H, Bray F, Jemal A, Yu XQ and He J: Cancer statistics in China, 2015. *CA Cancer J Clin* 66: 115-132, 2016.
- Zong L, Abe M, Seto Y and Ji J: The challenge of screening for early gastric cancer in China. *Lancet* 388: 2606, 2016.
- Johnson LA and June CH: Driving gene-engineered T cell immunotherapy of cancer. *Cell Res* 27: 38-58, 2017.
- Essand M and Loskog AS: Genetically engineered T cells for the treatment of cancer. *J Intern Med* 273: 166-181, 2013.
- Batlevi CL, Matsuki E, Brentjens RJ and Younes A: Novel immunotherapies in lymphoid malignancies. *Nat Rev Clin Oncol* 13: 25-40, 2016.
- Wei SM: Monoclonal antibodies against gastric cancer and their selective reaction on various tissues. *Zhonghua Zhong Liu Za Zhi* 11: 162-164, 1989 (In Chinese).
- Xu G, Zhang M, Liu B, Li Z, Lin B, Xu X, Jin M, Li J, Wu J, Dong Z *et al*: Radioimmunoguided surgery in gastric cancer using 131-I labeled monoclonal antibody 3H11. *Semin Surg Oncol* 10: 88-94, 1994.
- Wang C, Wang Y, Su X, Lin B, Xu X, Zhang M, Li J and Xu G: Iodine-125 labeled monoclonal antibody 3H11: In radioimmunoguided surgery for primary gastric cancer. *Zhonghua Wai Ke Za Zhi* 38: 507-509, 2000 (In Chinese).
- Li J, Wang Y, Li QX, Wang YM, Xu JJ and Dong ZW: Cloning of 3H11 mAb variable region gene and expression of 3H11 human-mouse chimeric light Chain. *World J Gastroenterol* 4: 41-44, 1998.
- Chen D and Shou C: Molecular cloning of a tumor-associated antigen recognized by monoclonal antibody 3H11. *Biochem Biophys Res Commun* 280: 99-103, 2001.
- Liu X, Ory V, Chapman S, Yuan H, Albanese C, Kallakury B, Timofeeva OA, Nealon C, Dakic A, Simic V, *et al*: ROCK inhibitor and feeder cells induce the conditional reprogramming of epithelial cells. *Am J Pathol* 180: 599-607, 2012.
- Ye J, Ma N, Madden TL and Ostell JM: IgBLAST: An immunoglobulin variable domain sequence analysis tool. *Nucleic Acids Res* 41 (Web Server Issue): W34-W40, 2013.
- Enblad G, Karlsson H and Loskog AS: CAR T-Cell therapy: The role of physical barriers and immunosuppression in lymphoma. *Hum Gene Ther* 26: 498-505, 2015.
- Tang XY, Sun Y, Zhang A, Hu GL, Cao W, Wang DH, Zhang B and Chen H: Third-generation CD28/4-1BB chimeric antigen receptor T cells for chemotherapy relapsed or refractory acute lymphoblastic leukaemia: A non-randomised, open-label phase I trial protocol. *BMJ Open* 6: e013904, 2016.
- Ozawa K: Current status and future development of CAR-T gene therapy. *Rinsho Ketsueki* 56: 2180-2185, 2015 (In Japanese).
- Davenport AJ, Jenkins MR, Ritchie DS, Prince HM, Trapani JA, Kershaw MH, Darcy PK and Neeson PJ: CAR-T cells are serial killers. *Oncoimmunology* 4: e1053684, 2015.
- Schneider U, Schwenk HU and Bornkamm G: Characterization of EBV-genome negative 'null' and 'T' cell lines derived from children with acute lymphoblastic leukemia and leukemic transformed non-Hodgkin lymphoma. *Int J Cancer* 19: 621-626, 1977.
- Kobayashi E, Kishi H, Ozawa T, Hamana H, Nakagawa H, Jin A, Lin Z and Muraguchi A: A chimeric antigen receptor for TRAIL-receptor 1 induces apoptosis in various types of tumor cells. *Biochem Biophys Res Commun* 453: 798-803, 2014.
- Shirasu N, Shibaguci H, Kuroki M, Yamada H and Kuroki M: Construction and molecular characterization of human chimeric T-cell antigen receptors specific for carcinoembryonic antigen. *Anticancer Res* 30: 2731-2738, 2010.
- Jamnani FR, Rahbarizadeh F, Shokrgozar MA, Mahboudi F, Ahmadvand D, Sharifzadeh Z, Parhamifar L and Moghimi SM: T cells expressing VHH-directed oligoclonal chimeric HER2 antigen receptors: Towards tumor-directed oligoclonal T cell therapy. *Biochim Biophys Acta* 1840: 378-386, 2014.
- Khaleghi S, Rahbarizadeh F, Ahmadvand D, Rasaei MJ and Pognonec P: A caspase 8-based suicide switch induces apoptosis in nanobody-directed chimeric receptor expressing T cells. *Int J Hematol* 95: 434-444, 2012.
- Zhang Q, Wang H, Li H, Xu J, Tian K, Yang J, Lu Z and Zheng J: Chimeric antigen receptor-modified T Cells inhibit the growth and metastases of established tissue factor-positive tumors in NOG mice. *Oncotarget* 8: 9488-9499, 2017.
- Pule MA, Savoldo B, Myers GD, Rossig C, Russell HV, Dotti G, Huls MH, Liu E, Gee AP, Mei Z, *et al*: Virus-specific T cells engineered to coexpress tumor-specific receptors: Persistence and antitumor activity in individuals with neuroblastoma. *Nat Med* 14: 1264-1270, 2008.
- Zuccolotto G, Fracasso G, Merlo A, Montagner IM, Rondina M, Bobisse S, Figini M, Cingarlini S, Colombatti M, Zanovello P and Rosato A: PSMA-specific CAR-engineered T cells eradicate disseminated prostate cancer in preclinical models. *PLoS One* 9: e109427, 2014.
- Craddock JA, Lu A, Bear A, Pule M, Brenner MK, Rooney CM and Foster AE: Enhanced tumor trafficking of GD2 chimeric antigen receptor T cells by expression of the chemokine receptor CCR2b. *J Immunother* 33: 780-788, 2010.
- Caruana I, Savoldo B, Hoyos V, Weber G, Liu H, Kim ES, Ittmann MM, Marchetti D and Dotti G: Heparanase promotes tumor infiltration and antitumor activity of CAR-redirection T lymphocytes. *Nat Med* 21: 524-529, 2015.



This work is licensed under a Creative Commons Attribution-NonCommercial-NoDerivatives 4.0 International (CC BY-NC-ND 4.0) License.